Annals of Botany **121**: 297–310, 2018
doi:10.1093/aob/mcx160, available online at www.academic.oup.com/aob

ANNALS OF BOTANY
Founded 1887

The *Arabidopsis thaliana* non-specific phospholipase C2 is involved in the response to *Pseudomonas syringae* attack

Zuzana Krčková[1], Daniela Kocourková[1], Michal Daněk[1], Jitka Brouzdová[1], Přemysl Pejchar[1], Martin Janda[1,4], Igor Pokotylo[2], Peter G. Ott[3], Olga Valentová[4] and Jan Martinec[1,*]

[1]Institute of Experimental Botany of the Czech Academy of Sciences, Czech Republic, [2]The Institute of Bioorganic Chemistry and Petrochemistry, National Academy of Sciences of Ukraine, Ukraine, [3]Plant Protection Institute, Centre for Agricultural Research, Hungarian Academy of Sciences, Hungary and [4]Department of Biochemistry and Microbiology, University of Chemistry and Technology, Prague, Czech Republic
**For correspondence. E-mail martinec@ueb.cas.cz*

Received: 3 July 2017 Returned for revision: 23 August 2017 Editorial decision: 10 October 2017 Accepted: 24 October 2017
Published electronically: 29 December 2017

• **Background and Aims** The non-specific phospholipase C (NPC) is a new member of the plant phospholipase family that reacts to abiotic environmental stresses, such as phosphate deficiency, high salinity, heat and aluminium toxicity, and is involved in root development, silicon distribution and brassinolide signalling. Six NPC genes (*NPC1–NPC6*) are found in the Arabidopsis genome. The NPC2 isoform has not been experimentally characterized so far.
• **Methods** The Arabidopsis NPC2 isoform was cloned and heterologously expressed in *Escherichia coli*. NPC2 enzyme activity was determined using fluorescent phosphatidylcholine as a substrate. Tissue expression and subcellular localization were analysed using GUS- and GFP-tagged NPC2. The expression patterns of *NPC2* were analysed via quantitative real-time PCR. Independent homozygous transgenic plant lines overexpressing *NPC2* under the control of a 35S promoter were generated, and reactive oxygen species were measured using a luminol-based assay.
• **Key Results** The heterologously expressed protein possessed phospholipase C activity, being able to hydrolyse phosphatidylcholine to diacylglycerol. NPC2 tagged with GFP was predominantly localized to the Golgi apparatus in Arabidopsis roots. The level of NPC2 transcript is rapidly altered during plant immune responses and correlates with the activation of multiple layers of the plant defence system. Transcription of *NPC2* decreased substantially after plant infiltration with *Pseudomonas syringae*, flagellin peptide flg22 and salicylic acid treatments and expression of the effector molecule AvrRpm1. The decrease in *NPC2* transcript levels correlated with a decrease in NPC2 enzyme activity. NPC2-overexpressing mutants showed higher reactive oxygen species production triggered by flg22.
• **Conclusions** This first experimental characterization of NPC2 provides new insights into the role of the non-specific phospholipase C protein family. The results suggest that NPC2 is involved in the response of Arabidopsis to *P. syringae* attack.

Key words: *Arabidopsis thaliana*, non-specific phospholipase C, phosphatidylcholine-specific phospholipase C, *Pseudomonas syringae*, MAMP-triggered immunity, effector-triggered immunity, reactive oxygen species, flagellin

INTRODUCTION

Phospholipases are the key components of the plant phospholipid signalling network, which regulates numerous physiological processes as well as responses to biotic and abiotic stress factors. The phospholipid signalling network includes, among others, phospholipid-metabolizing enzymes phospholipase C (PLC), phospholipase D (PLD), and phospholipases A_1 and A_2. PLCs cleave membrane phospholipids, releasing water-soluble phosphorylated headgroups and diacylglycerol (DAG). PLCs can be generally grouped according to substrate specificity into phosphatidylinositol-specific phospholipases C (PI-PLCs) and phosphatidylcholine-specific phospholipases C (PC-PLCs). PC-PLCs, which are also referred to in plants as non-specific PLCs (NPCs), are characterized by broader substrate ranges that include the most abundant membrane lipid phosphatidylcholine (PC). In addition to their signalling functions, phospholipases also play a role in lipid metabolism.

Based on sequence similarity with bacterial PC-PLC, six NPC genes (*NPC1–NPC6*) were identified in the Arabidopsis genome. Later, NPC genes were found in rice (Singh *et al.*, 2013) and cotton (Zhang *et al.*, 2017). NPC1 was localized to secretory pathway compartments in Arabidopsis roots (Krčková *et al.*, 2015). NPC4 was found to be a plasma membrane-bound protein (Nakamura *et al.*, 2005; Gaude *et al.*, 2008; Peters *et al.*, 2014; Pejchar *et al.*, 2015). NPC5 is a cytosolic enzyme expressed only in floral organs under some physiological conditions (Gaude *et al.*, 2008; Peters *et al.*, 2010; Wimalasekera *et al.*, 2010). NPC1, NPC4 and NPC5 hydrolyse PC (Gaude *et al.*, 2008;

Krčková *et al.*, 2015). Reddy *et al.* (2010) described NPC3 as an enzyme that has lysophosphatidic acid phosphatase activity instead of PLC activity. NPC2 and NPC6, which have not been experimentally characterized so far, are reported to contain putative N-terminal signal peptides and are predicted to localize to endomembranes and specific organelles (Pokotylo *et al.*, 2013).

Recent research has revealed important roles for Arabidopsis NPCs as mediators of plant metabolism in relation to phospholipid-to-galactosyl DAG exchange (Andersson *et al.*, 2005; Nakamura *et al.*, 2005; Gaude *et al.*, 2008; Tjellström *et al.*, 2008), in growth and development related to hormone signalling (Peters *et al.*, 2010; Wimalasekera *et al.*, 2010) and in stress responses to changing environmental conditions (Scherer *et al.*, 2002; Pejchar *et al.*, 2010, 2015; Kocourková *et al.*, 2011; Peters *et al.*, 2014; Krčková *et al.*, 2015; Pejchar and Martinec, 2015). *Os*NPC1 was found to modulate silicon distribution and secondary cell-wall deposition in rice nodes and grains (Cao *et al.*, 2016).

Plants, as sessile organisms, have evolved sophisticated and wide-ranging strategies to survive biotic stresses imposed by pathogens. Plants do not possess dedicated immune cells and, in the case of infection, rely on cell-autonomous events (Spoel and Dong, 2012). As a first line of passive defence, plants make use of mechanical barriers and constitutive production of antimicrobial secondary metabolites. However, upon contact with a pathogen, plants can promptly react and activate inducible defence mechanisms. Plants sense pathogen attack via conserved extracellular chemical structures, which include microbe-associated molecular pattern (MAMPs; e.g. lipopolysaccharides, flagellin and chitin) and damage-associated molecular patterns (components of breached cells) that stimulate MAMP-triggered immunity (PTI). In addition, specialized effector molecules, which are commonly secreted by pathogens into a host cell to suppress PTI, can also be sensed by plants and elicit the activation of effector-triggered immunity (ETI). Activation of both PTI and ETI is followed by production of reactive oxygen species (ROS; Senthil-Kumar and Mysore, 2013). PTI triggers ROS production, which typically occurs within minutes, whereas ETI is usually followed by a sustained production of ROS that is associated with the establishment of the hypersensitive response (HR; Torres, 2010). It has been shown that various isoforms of phospholipase D are involved in regulation of ROS production during plant–microbe interactions (Zhao, 2015).

Phospholipases are known to participate in plant defence reactions (Viehweger *et al.*, 2006; Vossen *et al.*, 2010; Janda *et al.*, 2013; Zhao *et al.*, 2013). Phospholipase D is involved in the signalling of the defence-related hormones salicylic acid (SA; Janda *et al.*, 2015; Krinke *et al.*, 2009) and jasmonic acid (JA; Wang *et al.*, 2000) by altering cell lipid metabolism, leading to the production of signalling molecules. Phospholipases have been shown to be associated with the establishment of systemic acquired resistance and induced systemic resistance responses (Profotová *et al.*, 2006). The addition of neomycin, which binds PI-PLC substrates, e.g. phosphatidylinositol phosphates, blocks the development of the HR in Arabidopsis plants expressing the bacterial AvrRpm1 effector (Andersson *et al.*, 2006). In contrast, the expression of some phospholipases seems to favour the propagation of infection, as was shown for patatin-like phospholipase 2 (PLP2) from Arabidopsis (La Camera *et al.*, 2005). The suppression of *OsPLDβ1* from rice also granted resistance to *Pyricularia grisea* and *Xanthomonas oryzae* pv. *oryzae* (Yamaguchi *et al.*, 2009). Recently, it was shown that PLDβ1 also plays both positive and negative roles in the defence responses of Arabidopsis. PLDβ1-deficient plants were characterized by enhanced resistance towards biotrophic *Pseudomonas syringae* and induced expression of SA-dependent genes upon infection. At the same time, these mutants were more susceptible to the necrotrophic fungus *Botrytis cinerea* and accumulated less JA (Zhao *et al.*, 2013). A rapid decrease in the NPC-dependent production of DAG in tobacco VBI-0 cells was found after treatment with the elicitor cryptogein from *Phytophthora cryptogea* (Scherer *et al.*, 2002). These results indicate a divergent role for phospholipases in plant resistance.

In this study, we present the initial characterization and tissue-specific and intracellular localization of Arabidopsis NPC2. In addition, analysis of expression and enzyme activity levels demonstrate the involvement of NPC2 in the response to *P. syringae* attack and biotic stress-associated stimuli.

MATERIALS AND METHODS

Plant materials

Arabidopsis thaliana Columbia (Col-0) seeds were obtained from Lehle seeds (Round Rock, TX, USA) and used as wild-type controls. T-DNA insertion line *npc2* (SALK_018011, SIGNAL collection; Alonso, 2003) was used in the experiments. T-DNA insertion was confirmed by PCR, using left border primer LBb1 5′-GCGTGGACCGCTTGCTGCAACT-3′ and oligonucleotides 5′-TTCAACAAGCATATTCCGAGG-3′, 5′-GAGGGTGTCCATGTAACGTTG-3′. All PCRs were performed with PPP Master Mix (Top-Bio, Prague, Czech Republic). Several Wave lines were purchased from NASC (http://arabidopsis.info/), and the presence of the mCherry-labelled marker in their genome was verified as described previously (Geldner *et al.*, 2009). Wave_127R line (NASC ID: N781684), encoding MEMB12 (At5g50440) fused with mCherry, was then crossed with the 35S::NPC2:GFP line, and the F_1 generation was observed.

Plants overexpressing *NPC2* were prepared as follows. *NPC2* was amplified from Arabidopsis Col-0 cDNA using specific primers (forward 5′-CGAGTCGACAATGTCT ATT AAAGCATTTGCTTT-3′, reverse 5′-TATGCGGCCGCTTTTAA GGTCTTCTTCCGGTG-3′), cloned into the pENTR3C entry vector (Invitrogen, Carlsbad, CA, USA) and recombined by the LR reaction into the Gateway binary vector pGWB2 (Nakagawa *et al.*, 2007) under the control of the CaMV 35S promoter. *pNPC2:GUS* plants were prepared as follows. The putative NPC2 promoter (whole intergenic region – an approx. 550-bp genomic sequence upstream of the start codon of *NPC2*) was amplified from Arabidopsis Col-0 genomic DNA using specific primers (forward 5′-CCAGTCGACTATTTGTGCT AATCTTTTTTACCTTCA-3′, reverse 5′-TATGCGGCCG CTTTGTT TTGGGGGAATGGTAG-3′), cloned into the pENTR3C entry vector (Invitrogen) and recombined by the LR reaction into the Gateway binary vector pKGWFS7 (Karimi *et al.*, 2002). Final constructs were transferred into *Agrobacterium tumefaciens* strain GV2260, and Arabidopsis Col-0 wild-type plants were transformed by the floral dip method (Clough and Bent, 1998). Transformants were selected on agar plates

containing 50 µg mL^{-1} kanamycin and 50 µg mL^{-1} hygromycin B. Expression levels of *NPC2* in the T3 seedlings of homozygous lines were measured using quantitative (q)RT-PCR. Plants expressing AvrRpm1 under the control of the dexamethasone-inducible promoter in Col 0, *rpm1.3* and *rpm1.3 rps2-101C* backgrounds, as well as *rpm1.3* (Grant *et al.*, 1995), *rpm1.3 rps2-101C* (Mindrinos *et al.*, 1994) null mutants, were obtained from David Mackey (Ohio State University, USA). Mutants *npr1-1*, *sid2-3*, NahG and *fls2* were obtained from Vladimír Šašek (IEB, Czech Academy of Sciences, Czech Republic; Sasek *et al.*, 2014). Plants were grown in Jiffy 7 peat soil pellets for 4–5 weeks. A 10-h/14-h light (100 µmol m^{-2} s^{-1})/dark cycle at 75 % relative humidity and day/night temperatures of 22 and 20 °C, respectively, were used.

Bacteria

Bacterial strains *P. syringae* pv. *maculicola* (*Psm*) strain 4326, *Psm* 4326 AvrRpm1 (strain expressing the AvrRpm1 gene), *P. syringae* pv. *tomato* (*Pst*) strain DC3000, *Pst* DC3000 COR$^-$ (coronatine-deficient mutant) and *Pst* DC3000 *hrcC*$^-$ (mutant deficient in the type-III secretion system) were used. Bacterial suspensions at the indicated densities [from 10^6 to 10^{10} colony forming units (cfu) mL^{-1}] were infiltrated into leaves with a needleless syringe. To determine number of bacteria, four leaf discs (diameter 0.7 mm) were ground, and the bacteria number was counted in serial 1: 10 dilutions.

Cloning

The cDNA of NPC2 (At2g26870) was amplified from Arabidopsis using specific primers (5′-GCGCTCGAGTTAAGGT CTTCTTCCGGTG-3′ and 5′- GCCGATATCATGACAAGTC CGATCAAAACCA-3′). The PCR product was digested with *Xho*I and *Eco*RV, and directly ligated in-frame into the expression vector pET-30a(+) (pET30; Novagen) with a 6xHis tag. The presence and sequence of the gene in the resulting plasmid was confirmed by sequencing.

Protein production

The construct coding for the fusion protein was transformed into *Escherichia coli* strain ArcticExpress (DE3) cells. The expression of recombinant protein was induced by adding 0.1 mM isopropyl β-thio-galactopyranoside when the OD_{600} of culture reached approx. 0.4. The production lasted for 24 h at 13 °C and 120 rpm.

The cells were harvested by centrifugation (5000 *g*, 10 min), re-suspended in lysis buffer (50 mM NaH_2PO_4, 300 mM NaCl, 30 mM imidazol) and sonicated after 10 min treatment with lysozyme (1 mg mL^{-1}). The lysed cell suspension was centrifuged (10 000 *g*, 10 min), and the supernatant was purified on Ni-NTA agarose (Qiagen, Valencia, CA, USA) according to the manufacturer's instructions, desalted on a PD-10 column (GE Healthcare, Little Chalfont, UK) using desalting buffer [50 mM 2-(*N*-morpholino)ethanesulfonic acid (MES), 300 mM NaCl] and concentrated with Vivaspin ultrafiltration spin columns (Sartorius Stedim, Göttingen, Germany). Purified protein was used for the enzyme activity assays.

NPC activity assay in vitro

Arabidopsis proteins NPC2, NPC4 and empty vector pET30 as a control were expressed in *E. coli* and their enzyme activities were measured *in vitro*. Protein concentration was determined by the method of Bradford (1976). The substrate solution contained 0.66 µg of fluorescent phosphatidylcholine (bodipy-PC, D-3771, Invitrogen), 3.57 µg of 1,2-dipalmitoyl-sn-glycerol-3-phosphocholine (850355C, Avanti Polar Lipids, Alabaster, AL, USA) and 0.0625 µg of sodium deoxycholate (302-95-4, MP Biomedicals, USA) in 25 µL of MES buffer (200 mM, pH 6.5). This substrate solution was gently mixed for 30 min at room temperature and then sonicated for 10 min. The reaction was initiated by mixing of 75 µL of protein sample (total protein amount 20 µg) with 25 µL of substrate solution. The reaction proceeded for 4 h at 16 °C with shaking at 300 rpm. Lipids were extracted, and DAG, the product of NPC activity, was quantified according to Pejchar *et al.* (2013) with some modifications. The enzyme reaction was stopped by the addition of 400 µL of cold methanol/chloroform (2: 1, v/v). After 30 min, 200 µL KCl (0.1 M) was added to the stopped reaction mixture and mixed again. The lower phase (110 µL) was evaporated and re-dissolved in 50 µL of ethanol. Samples were analysed by high-performance thin layer chromatography (HP-TLC) on silica gel-60 plates (Merck KGaA, Darmstadt, Germany). Plates were developed in a mobile phase of methanol/chloroform/water (25: 65: 4, by vol.), dried and visualized using a Fuji FLA-7000 fluorescence scanner (Fujifilm, Tokyo, Japan). The identification of the lipid spots corresponding to bodipy-lipid was based on a comparison with the bodipy-lipid standards (Pejchar *et al.*, 2010).

Histochemical β-glucuronidase (GUS) staining

The histochemical GUS assay (Jefferson *et al.*, 1987) was carried out on plants grown on agar plates (7-, 10-, 14-d-old seedlings) and in Jiffy peat soil pellets (5-week-old plants). The seedlings and plant parts were immersed in X-Gluc buffer [2 mM X-Gluc, 50 mM $NaPO_4$, pH 7, 0.5 % (v/v) Triton-X, 0.5 mM K-ferricyanide] for 16 h at 37 °C. Chlorophyll was removed by repeated washing in 80 % (v/v) ethanol. Observations were made on a Nikon SMZ 1500 zoom stereoscopic microscope coupled to a Nikon DS-5M digital camera.

Confocal microscopy

For microscopic observations, 5-d-old seedlings grown on vertical 1 % agar plates (Duchefa, Amsterdam, the Netherlands; pH 5.8) containing ½ Murashige-Skoog (MS) salt and 1 % sucrose were used. Plasma membrane labelling was performed by incubating the seedlings in ½ MS + 1 % sucrose liquid medium containing 2 µM FM4-64 [*N*-(3-triethylammoniumpropyl)-4-(6-(4-(diethylamino) phenyl) hexatrienyl) pyridinium dibromide] on ice for 5 min. For endosome labelling, seedlings were incubated in the same medium at room temperature for 10 min.

Seedlings were then mounted in ½ MS + 1 % sucrose liquid medium on microslides and observed using a 63× objective (Plan-Apochromat NA = 1.4, oil immersion; Zeiss, Oberkochen, Germany) on a Zeiss 880 laser scanning confocal microscope. For GFP fluorescence acquisition, 488 nm laser excitation was used and 493–540 nm emission was collected. For FM4-64 and mCherry excitation, a 561-nm laser was used. Emission was collected within 605–700 or 595–670 nm for FM4-64 and mCherry, respectively. For co-localization imaging, the two channels were collected simultaneously to avoid changes of puncta positions during delays in single channel acquisition. The signals were well separated, having been checked in single-label specimens where no bleed-through was detected between channels when the above-described emission detection settings were applied.

Microarray expression data collection and processing

The *NPC2* microarray expression data were obtained using the Genevestigator interface (Hruz *et al.*, 2008). Data demonstrating *NPC2* expression changes were monitored at the $P < 0.05$ significance level in the *A. thaliana* Columbia (Col-0) genetic background. The experimental conditions that induced *NPC2* expression changes that were more than 1.5-fold (either upregulation or downregulation) were noted and reproduced as a graphical figure. The descriptions of the experimental conditionsused for microarrays are provided in the Supplementary Data (Table S1).

Quantitative RT-PCR

For expression analyses, 4–5-week-old plants at the rosette leaf stage were used. Bacterial suspensions (10^6, 10^7, 10^8 or 10^9 cfu mL^{-1}), 1 µM flg22 (22-amino acid peptide from N-terminal part of flagellin, GenScript, Piscataway, NJ, USA, cat. no. RP19986), 500 µM SA, 50 µM methyljasmonic acid (MeJA) and 5 mM 1-aminocyclopropane-1-carboxylic acid (ACC), or water were infiltrated to the leaves. Leaf samples were collected at the indicated time points (1, 3, 6, 12, 24 or 36 h) after infiltration. The expression of each gene in water-infiltrated controls at the respective times was set to 1. AvrRpm1 expression in plants was induced by spraying plants with 20 µM dexamethasone containing 0.005 % Silwet L-77. Samples were collected 16 h after induction. The expression of *NPC2* in 0.005 % Silwet L-77-sprayed controls at the respective times was set to 1. The leaf samples were immediately frozen in liquid nitrogen. RNA was isolated using a Spectrum Plant Total RNA Kit (Sigma-Aldrich, St Louis, MO, USA), a Turbo DNA-free Kit (Applied Biosystems) was used for DNA removal, and a Transcriptor High Fidelity cDNA Synthesis Kit (Roche, Indianapolis, IN, USA) was used for cDNA synthesis. The reverse transcription reaction was primed with anchored-oligo(DT)18 primers. qRT-PCR was performed with a LightCycler480 system (Roche) using the LightCycler480 SYBR Green I Master (Roche). *NPC2* expression was detected with primers 5′-TCTC CGAGTTCGCTGTTTTC-3′ and 5′-TGACGTCCCTGAGTG TACAAA-3′. SAND (At2g28390) was used as a reference gene for the normalization of target gene expression (5′-GGA TTTTCAGCTACTCTT CAAGCTA-3′, 5′-CTGCCTTGACTA AGTTGACACG-3′; Czechowski *et al.*, 2005). The fold change in the expression of the target gene was calculated according to Pfaffl *et al.* (2001). Transcripts of other *NPC* isoforms were detected according to Kocourková *et al.* (2011).

Preparation of protoplasts

Protoplasts from Arabidopsis leaves were prepared according to the methods of Wu *et al.* (2009) from 5-week-old plants. Briefly, the peeled leaves were incubated in enzyme solution [1 % cellulase Onozuka R10, 0.25 % macerozyme Onozuka R10 (both Yakult, Japan), 0.1 % bovine serum albumin, 0.4 M mannitol, 10 mM $CaCl_2$, 20 mM KCl, 20 mM MES, pH 5.7) for 1 h with gentle shaking at 40 rpm. Protoplasts were centrifuged at 100 *g* for 3 min and washed twice with 25 mL modified W5 solution (154 mM NaCl, 125 mM $CaCl_2$, 5 mM glucose, 5 mM KCl, 2 mM MES, pH 5.7). Protoplasts were then counted, diluted to the desired concentration in W5 solution and incubated for 1 h at room temperature prior to the experiment.

NPC activity in Arabidopsis protoplasts

Isolated protoplasts in modified W5 solution were used at a final concentration of approx. 3×10^3 protoplasts mL^{-1}. Protoplasts in a final volume of 1 mL were treated on an orbital shaker (125 rpm) with 1 µM flg22 or 200 µM SA for 1, 3 or 6 h at 23 °C under white light (30 µmol m^{-2} s^{-1}). Protoplasts were labelled with 0.66 µg mL^{-1} of bodipy-PC 30 min before the end of treatment. Lipids were extracted, and DAG was quantified according to the methods of Pejchar *et al.* (2013). Briefly, the enzyme reaction was stopped, and lipids were extracted by the addition of 4 mL of cold methanol/chloroform (2: 1, v/v). Extracted lipids were applied on HP-TLC silica gel-60 plates and analysed as described above.

Measurement of ROS production

ROS production was determined by the luminol-based assay as described with modifications (de Jonge *et al.*, 2010; Sasek *et al.*, 2014). Discs, 3 mm in diameter, were cut from the fully developed leaves (two discs per leaf) of 4-week-old Arabidopsis plants (three leaves per plant). Discs were incubated in 96-well plates in 150 µL distilled water for 16 h. The distilled water was replaced with 200 µL of reaction solution containing 17 µg mL^{-1} of luminol, 10 µg mL^{-1} of horseradish peroxidase (Sigma, P-8125) and 100 nM flg22. The measurement was performed with a luminometer immediately after adding the flg22 (Tecan infinite F200) for a period of 30 min.

RESULTS

AtNPC2 encodes a PLC that hydrolyses phosphatidylcholine

To uncover whether the NPC2 gene encodes a functional phospholipase, NPC2 protein was expressed in *E. coli* and purified using His-tag.

Recombinant NPC2 was prepared by inserting AtNPC2 cDNA into the expression vector pET30. The cleavage site between the signal peptide and the coding region was identified using SignalP 4.1, and the signal sequence was removed. Removal of signal sequence was essential for enzyme activity of recombinant NPC2. Sufficient production of soluble NPC2 was obtained using *E. coli* ArcticExpress (DE3) cells, which can grow at low temperatures. Protein was purified on Ni-NTA agarose, desalted to remove imidazole and concentrated. The purification process was monitored by Western blot using anti-His-tag antibodies. We also prepared recombinant NPC4, the cloning, production and activity of which has been described (Nakamura *et al.*, 2005). NPC4 served as a positive control of our purification process as well as phospholipase activity measurement. Protein bands detected with the antibody corresponding to the size of NPC2 (60 kDa) and NPC4 (65 kDa) were identified. The empty vector pET30 served as a negative control (Fig. 1A).

The phospholipase activity of purified proteins was tested using a bodipy-PC as a substrate (Pejchar *et al.*, 2013). Lipids were extracted and separated by HP-TLC, and fluorescently labelled products were detected. The results showed that NPC2 can produce DAG from PC. The expressed NPC4 showed the same activity, whereas the negative control (the empty vector) had no activity (Fig. 1B). Lysophosphatidylcholine, the product of phospholipase A activity, was detected in NPC samples as well as in a negative control sample, which points to a possible co-purification of phospholipase A.

According to these results, NPC2 was shown to encode a functional phosphatidylcholine-hydrolysing PLC.

Tissue-specific localization of NPC2 *transcript*

To reveal tissue-specific expression patterns, we prepared Arabidopsis plants stably transformed with putative AtNPC2 promoter:GUS transcriptional fusions and used a histochemical GUS assay. GUS staining of plant organs at several developmental stages revealed that *NPC2* was expressed in a wide range of plant organs (Fig. 2). The intensity of GUS staining was similar throughout seedling development (Fig. 2A–C). In adult plants, GUS activity in the inflorescence and siliques was relatively high, similar to seedlings (Fig. 2D–F). In both young and old leaves of adult plants, GUS activity was weaker than in seedlings (Fig. 2G, H,). In the root system, expression of pNPC2:GUS was highest at root tips and lateral roots (Fig. 2I, J). In young leaves, only hydathodes were clearly stained (Fig. 2G).

NPC2 *is localized to Golgi apparatus*

To determine the subcellular localization of NPC2, stable transformants of 4–5-d-old Arabidopsis seedlings expressing NPC2:GFP fusion protein under control of the CaMV 35S promotor were used. GFP signal was detected in root tissues, with the highest levels in root epidermis. In these cells, GFP

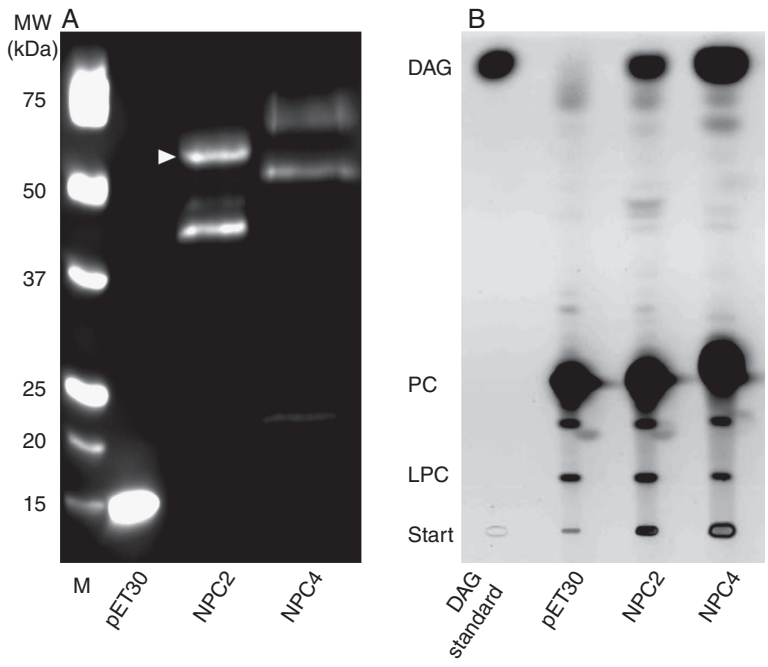

FIG. 1. Western blot analysis and *in vitro* activity of recombinant NPC2. (A) Western blot analysis of recombinant protein was performed under reducing conditions with SDS electrophoresis. 6xHis tag was detected with Anti-His HRP conjugate. In addition to a band of the correct size (~60 kDa, indicated by an arrowhead), other bands were observed, which are probably degradation products. (B) TLC image of bodipy-PC-derived reaction products with purified, heterologously expressed NPCs and empty vector. Proteins (20 µg in total) were incubated with bodipy-PC at 16 °C and shaken at 300 rpm for 4 h. Extracted lipids were separated by HP-TLC. NPC4 was used as a positive control and pET30 as a negative control. C, control-empty vector pET30a exhibiting the expression of a short protein with 6xHis tag; DAG, diacylglycerol; LPC, lysophosphatidylcholine; M, marker; PC, phosphatidylcholine.

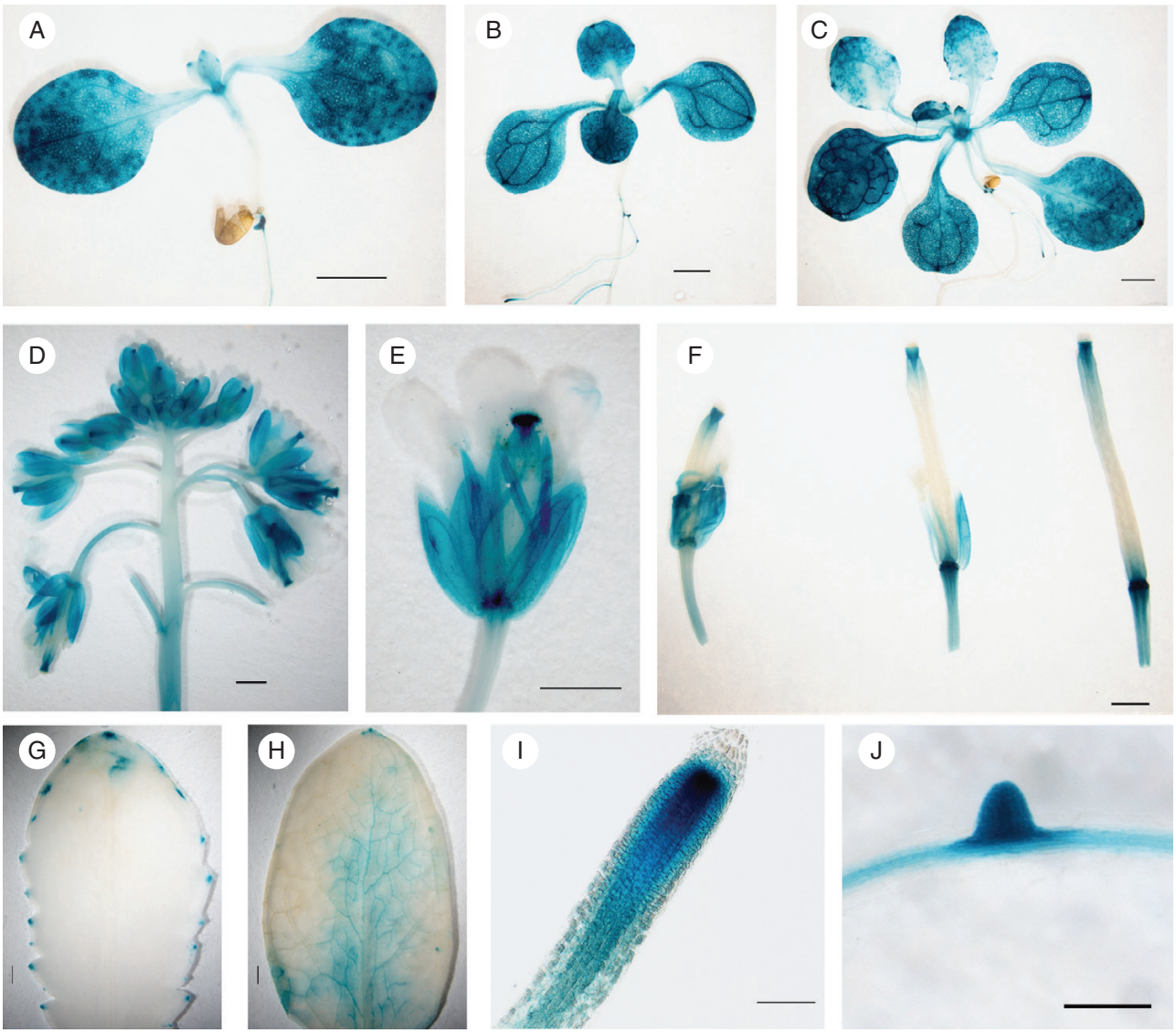

Fig. 2. Tissue-specific expression of *NPC2* by histochemical GUS reporter assay: (A) 7-d-old seedling, (B) 10-d-old seedling, (C) 14-d-old seedling, (D) inflorescence, (E) flower, (F) siliques, (G) young leaf, (H) old leaf (D–H, 5-week-old plants), (I) main root (14-d-old seedling), (J) lateral root (10-d-old seedling). Scale bars: A–C, E 1 mm; D, F, G, H 2 mm; I, J 0.1 mm.

fluorescence was present in the cytoplasm, mainly in the perinuclear and cortical cytoplasm. No co-localization with FM4-64-labelled plasma membrane was found (Fig. 3A–C). The cytoplasmic GFP signal consisted of fluorescence from aggregated puncta and reticulate structures (Fig. 3D). The fluorescence levels expressed as greyscale values converted into an RGB heat map and presented in Fig. 3E show that the puncta have relatively high fluorescence, whereas the reticular signal is very weak. We assume that the low signal corresponds to minor NPC2 localization on the endoplasmic reticulum (ER). To reveal the identity of the punctate signal, we first treated the roots with FM4-64 to label endosomal structures. Endocytosed FM4-64 is known to label endosomes, the *trans*-Golgi network, prevacuolar compartment and tonoplast (Bolte *et al.*, 2004). We observed minor co-localization of FM4-64-labelled endosomal structures with NPC2:GFP in root epidermal cells (Fig. 3F–K). We then crossed our 35S::NPC2:GFP line with several Wave lines (Geldner *et al.*, 2009) expressing mCherry-tagged protein markers for distinct secretion pathway compartments and looked for co-localization in F_1 seedlings. Prominent co-localization was found (Fig. 3L–Q) when crossed with Wave127 expressing MEMB12 specific for *cis*-Golgi cisternae (Uemura *et al.*, 2004).

Based on these findings, we conclude that NPC2 is present predominantly in the Golgi apparatus (GA) but also possibly (to a minor extent) in other compartments of the secretory pathway, such as ER or some post-Golgi compartments.

Expression of NPC2 *in response to stress conditions, hormone treatments, growth conditions and nutrients*

Analysis of microarray expression data provides an opportunity to predict a possible functional role of a target gene

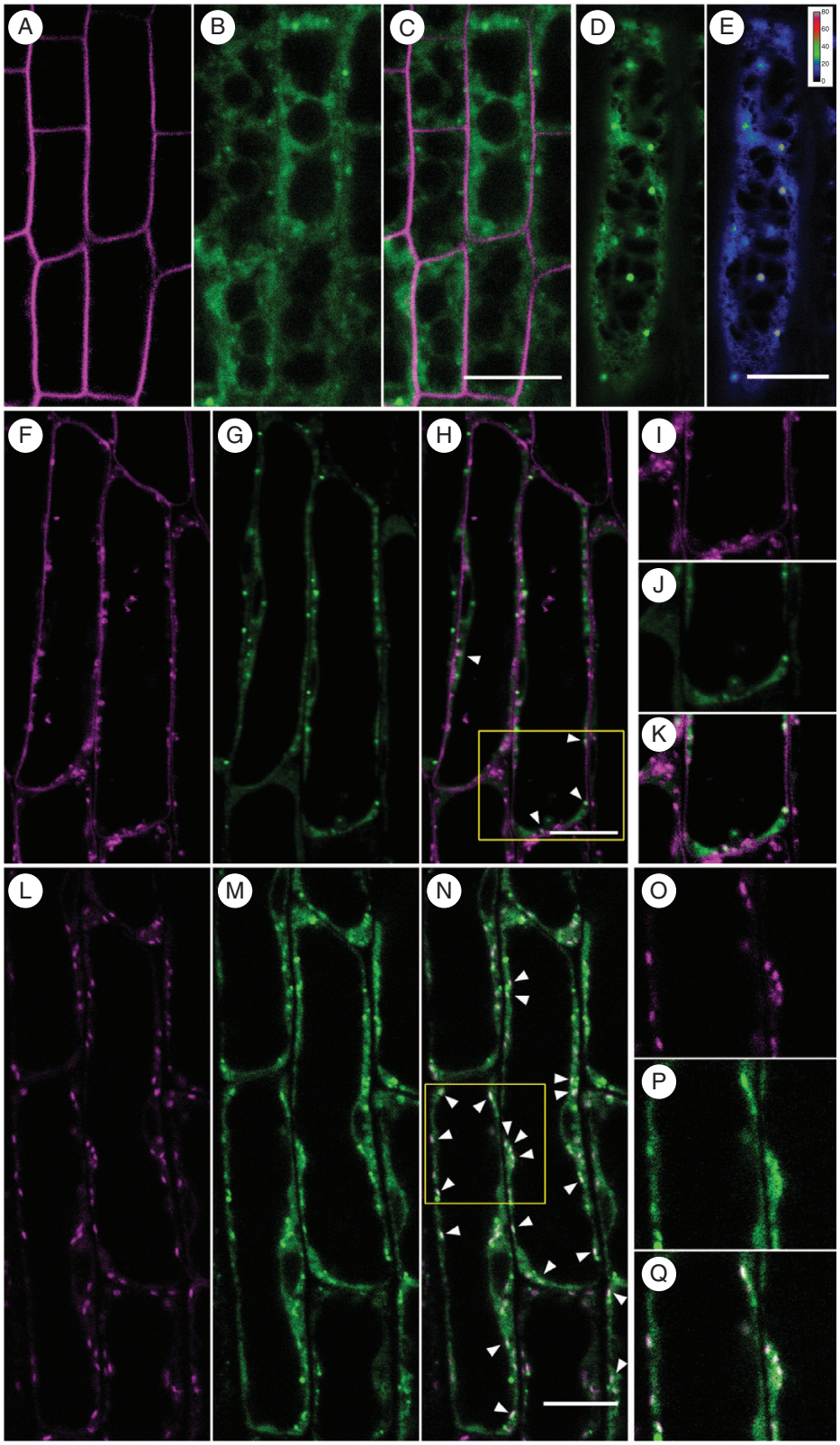

FIG. 3. Subcellular localization of 35S::NPC2:GFP in root epidermal cells of 5-d-old Arabidopsis seedlings. (A–C) FM4–64 was used to label plasma membranes and counter-stain cell borders. GFP fluorescence was detected in the cytoplasm, forming distinct puncta. (D, E) Besides the pronounced fluorescence in puncta, a weaker GFP signal was detected, suggesting possible endoplasmic reticulum localization. (F–H) FM4-64-labelled endosomes were found to colocalize to a minor extent with GFP puncta. (I–K) Close-up of the inset marked with a rectangle in H. (L–N) GFP puncta colocalized with MEMB12:mCherry marking Golgi apparatus. (O–Q) Close-up of the inset marked with a rectangle in N. (A, C, F, H, I, K) FM4-64 fluorescence in magenta. (B–E, G, J, K, M, N, P, Q) GFP fluorescence in green. (L, O, Q) mCherry fluorescence in magenta. Bars represent 10 μm.

within selected sets of stimuli. The data were obtained using the Genevestigator platform (Hruz *et al.*, 2008). The changes in abundance of Arabidopsis *NPC2* transcripts following abiotic stress treatments varied significantly depending on the stressor type, duration and plant organ (Fig. 4). The expression level of *NPC2* was steadily downregulated as a part of Arabidopsis responses to biotic attack. Bacterial or fungal pathogens, insect attack and treatment with harpin elicitor protein (HprZ) downregulated expression of *NPC2*. Notably, treatment with elicitor peptide 2 (Pep2) resulted in the induction of *NPC2* expression. However, unlike most elicitors, Pep2 is not a pathogen-derived molecule but produced *in planta* as a part of plant defence responses (Yamaguchi *et al.*, 2010). That is why its mode of action may differ from that of pathogen-secreted elicitors. The decrease of *NPC2* expression level was similarly observed following SA treatment, whereas no significant changes in *NPC2* transcript levels were reported in response to MeJA or ethylene.

Based on these facts, the level of *NPC2* expression and the specificity of NPC2 downregulation during Arabidopsis response to the biotrophic bacterial pathogen *P. syringae* were investigated in detail using qRT-PCR.

Expression of NPC2 *in response to* Psm

Arabidopsis plants were grown for 5 weeks and infiltrated with *Psm.* Using qRT-PCR, the expression of all members of the NPC gene family was measured in leaves 6 h after infiltration (10^8 cfu mL^{-1}). The most pronounced decrease in gene expression was ascribed to *NPC2* (Fig. 5A).

To further investigate the specificity of the expression pattern of *NPC2*, expression was measured for a shorter time span (1, 3 and 6 h after infiltration). Invariably, elevated suppression of *NPC2* expression was observed (Fig. 5B). Three hours after *Psm* infiltration (10^8 cfu mL^{-1}), the level of *NPC2* transcript decreased to 33 % of the untreated control. Suppressed *NPC2* expression persisted for a prolonged time span (12, 24 and 36 h after infiltration) as well (Supplementary Data Fig. S1A). We also investigated whether *NPC2* downregulation is dependent on the inoculum dose. A dependency on the bacterial dose used was observed (Fig. S1B). Notably, a decrease in the level of *NPC2* transcripts was observed even when the inoculum concentration was 10^6 cfu mL^{-1} (Fig. S1B).

Next, we investigated whether incompatible bacteria (*Psm* AvrRpm1), coronatine-deficient mutant bacteria (*Pst*COR$^-$) and bacteria that have an impaired type III secretion system (*Pst hrcC*$^-$) have the same effect on *NPC2* expression. We did not observe any significant differences in the decrease in *NPC2* expression in plants infiltrated with either *Psm* or *Pst* wild-types or with *Psm* AvrRpm1 or *Pst*COR$^-$ (Fig. S2A).

The reaction of Arabidopsis to *Pst hrcC*$^-$ at the level of *NPC2* expression depends on the time of sample collection. At early collection times (3 and 6 h), the *NPC2* transcript level did not differ from that of *Pst* wt-infiltrated plants. However, at a later time (24 h), the level of the *NPC2* transcript was restored nearly to the water-infiltrated control levels (Fig. S2B). Because the *Pst hrcC*$^-$ bacteria are not able to deliver effectors to the plant cell, these results suggest that at a later time, the downregulation of *NPC2* expression is a reaction to *Pst* bacterial effectors. In contrast, early changes in *NPC2* expression are likely to be activated by a MAMP-triggered pathway.

NPC2 *transcript level decreased during both PTI and ETI*

We used flg22 as a tool to specifically study the PTI response in Arabidopsis. We infiltrated 5-week-old Arabidopsis leaves with 1 µM flg22 and determined *NPC2* expression at 3, 6 and 24 h (Fig. 6A). The level of the *NPC2* transcript decreased after flg22 infiltration at early time points. Similarly to *Pst hrcC*$^-$ treatment, the level of the *NPC2* transcript at 24 h was higher than at 6 h (Fig. 6A). These results suggest that PTI-induced downregulation of NPC2 expression is transient.

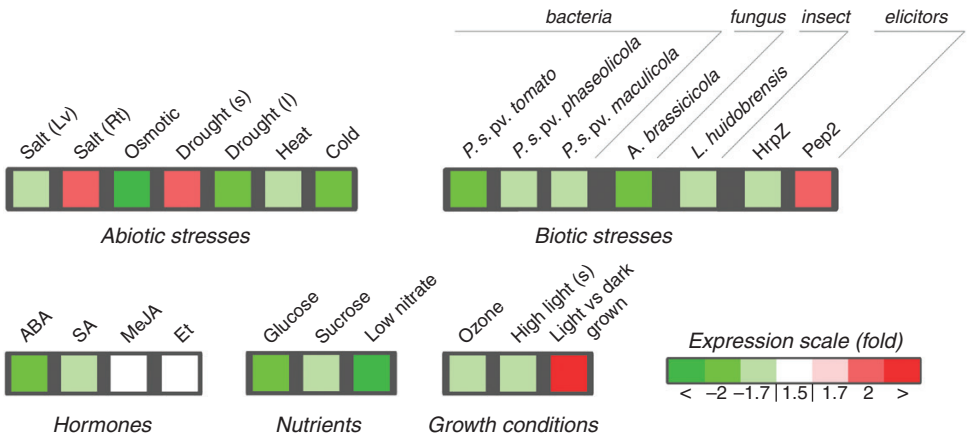

FIG. 4. NPC2 transcriptional response to environmental constrains, nutrients and hormonal treatments. Data were obtained by microarray analysis using the Genevestigator interface (https://genevestigator.com). *NPC2* expression level changes lower than 1.5-fold (either downregulation or upregulation) are shown in white. Selected conditions resulting in changes to *NPC2* expression level greater than 1.5-fold are shown in colour (red for upregulation, green for downregulation; scale is provided). For the description of experimental conditions used to collect microarray data, see Supplementary Data Table S1. Lv, leaves; Rt, roots; s, short treatment; l, long treatment; ABA, abscisic acid; SA, salicylic acid; MeJA, methyl jasmonate; Et, ethylene; HrpZ, harpin elicitor; Pep2, protein elicitor peptide 2; P.s., *Pseudomonas syringae*.

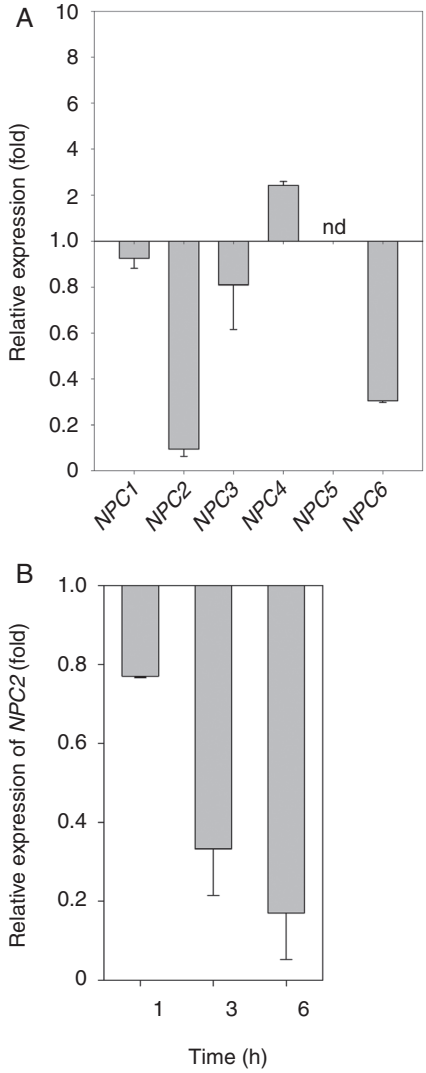

FIG. 5. Expression pattern of NPC genes in *Pseudomonas syringae* pv. *maculicola* (*Psm*)-treated plants. (A) Plants were treated with *Psm* (10^8 cfu mL^{-1}). The transcript levels of NPC genes were measured at 6 h after treatment by quantitative real-time PCR in leaves of 5-week-old plants. The expression of each gene in water-infiltrated controls was set to 1. *SAND* was used as a reference gene. The data represent the means ± s.e., $n = 4$ discrete samples from four biological experiments. (B) Detailed analysis of *NPC2* expression. The transcript level of *NPC2* was measured at 1, 3 and 6 h (10^8 cfu mL^{-1}) after *Psm* infiltration. The transcript level of the NPC2 gene in water-infiltrated controls at the respective times was set to 1. *SAND* was used as a reference gene. The data represent the means ± s.e., $n = 3$ discrete samples from three biological experiments. nd, Not detected; NPC, non-specific phospholipase C.

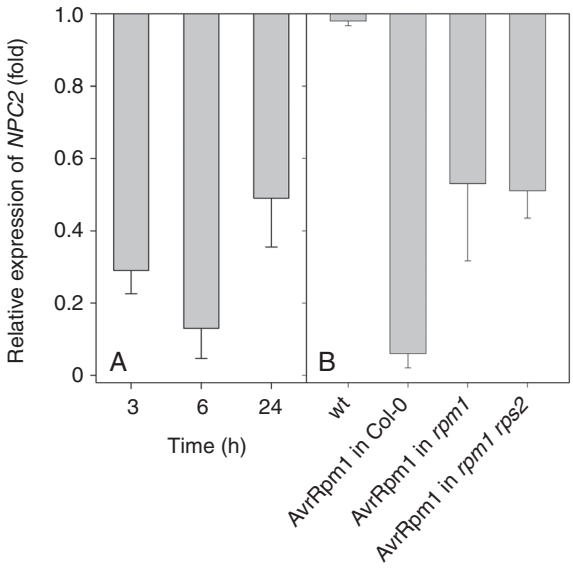

FIG. 6. Analysis of *NPC2* expression in flg22-infiltrated plants and in different transgenic plants expressing the effector AvrRpm1. (A) The transcript levels of the NPC2 gene were measured by quantitative real-time PCR in leaves infiltrated with 1 µM flg22 at the indicated times. (B) The leaves were sprayed with dexamethasone, and after 16 h transcript levels of the NPC2 gene were measured by quantitative real-time PCR. *SAND* was used as a reference gene. The expression of each gene in water-infiltrated (A) and sprayed (B) controls was set to 1. The data represent the means ± s.e., $n = 3$ discrete samples from three biological experiments. NPC2, non-specific phospholipase C2.

To study ETI without interference from the PTI pathway, we used Arabidopsis mutant plants in which expression of the effector molecule AvrRpm1 is controlled by dexamethasone-inducible promoter (Andersson *et al.*, 2006; Kim *et al.*, 2009). We tested plants expressing AvrRpm1 in the wt Col-0 background (Dex: AvrRpm1 Col 0), in the *RPM1* knockout mutant background (Dex: AvrRpm1 *rpm1*) and in the double mutant rpm*1 rps2* background (Dex: AvrRpm1 *rpm1 rps2*). In wt background plants, the effector protein AvrRpm1 activated both the RPM1 R-protein and RPS2 protein (Belkhadir *et al.*, 2004). At 16 h after dexamethasone treatment (20 µM), the *NPC2* transcript level was extensively reduced in all studied plant variants (Fig. 6B). The most apparent drop in the *NPC2* transcript level was in the case of AvrRpm1-expressing wt plants. This result is consistent with the observed decrease in the *NPC2* transcript level when Arabidopsis wt plants were infiltrated with the *Psm* AvrRpm1 bacteria, causing the ETI response (Fig. S2A). *NPC2* transcript levels also decreased to a lesser extent (6 % vs. 50 %) in both *rpm1* and *rpm1 rps2* background plants.

Decrease in NPC2 *transcript level is caused by SA and not by MeJA or ACC*

Pseudomonas syringae is a biotrophic pathogen that triggers defence responses, including the synthesis of SA (Spoel *et al.*, 2007). To determine whether SA alone and other phytohormones that are known to be involved in defence responses trigger a decrease in the *NPC2* transcript level, we infiltrated Arabidopsis leaves with SA (500 µM), MeJA (50 µM) and ACC (5 mM), which is a precursor of ethylene, and measured *NPC2* transcript levels at 3, 6 and 24 h after treatment. The only apparent reduction of *NPC2* transcript level was observed in plants treated with SA. MeJA and ACC treatments did not influence the *NPC2* transcript level (Fig. 7). The reduction was rapid and transient. The most obvious drop in the *NPC2* transcript level was detected 3 h after infiltration with SA. At 24 h after infiltration, the level of *NPC2* transcript was similar to mock-treated plants (Fig. 7). Expression of the following marker genes of individual hormone pathways was measured to confirm that the hormone treatments had stimulated the appropriate pathway: *PR1* (At2g14610) for SA, *PDF1.2* (At5g44420) for MeJA and

ERF1 (At3g23240) for ethylene pathways. The expression of marker genes was significantly upregulated after the corresponding treatments (data not shown).

Based on these results, we conclude that the decrease in the *NPC2* transcript level was triggered only by SA. Neither MeJA nor ACC triggered the *NPC2* expression response. This result is consistent with the experiment using *Pst*COR⁻ bacteria. Coronatine is a JA-mimicking substance, and there was no difference in *NPC2* expression in plants that were treated with *Pst* wt and *Pst*COR⁻ (Fig. S2A).

Enzyme activity of non-specific PLC is suppressed after flg22 and SA treatments

To determine whether the observed decrease in the *NPC2* transcript level is reflected by the level of enzymatic activity, protoplasts from leaves of 5-week-old Arabidopsis plants were treated with flg22 (1 μM) or SA (50 μM) for 1, 3 and 6 h. Protoplasts were used to gain higher reproducibility of the NPC activity measurements. We observed a similar decrease in the *NPC2* transcript level after flg22 and SA treatments in protoplasts as Arabidopsis leaves (data not shown). The quantity of bodipy-DAG, the product of NPC activity, remained the same after 1 h of SA and flg22 treatments (Fig. 8). However, the level of bodipy-DAG decreased to 75 % after 3 h of SA treatment and to 50 % after 3 h of flg22 treatment. The decrease in NPC activity was even greater after 6 h, at 59 % compared to non-treated control in the case of SA and 42 % in the case of flg22 treatment (Fig. 8). Because the decrease in enzymatic activity lags behind the downregulation of gene expression, we propose that the yet unknown function of NPC2 in biotic stress response is primarily controlled by transcription.

Plants overexpressing NPC2 *differ from wild-type plants in ROS production*

To investigate the function of NPC2 in response to *Psm* attack, we used a homozygous Arabidopsis T-DNA *npc2* knockout line (SALK 018011) and generated transgenic plants overexpressing *NPC2* under control of the 35S promoter. Transgenic plants were selected, and independent homozygous lines were obtained. Six lines, NPC2-OE23, NPC2-OE54, NPC2-OE62, NPC2-OE171, NPC2-OE295 and NPC2-OE325, each with a different level of overexpression from 3.4- to 20.7-fold (Fig. 9A), were selected for further study. No obvious phenotype differences were detected comparing wild type and the NPC-OE lines grown on either agar plates or soil.

NPC2 knockout and overexpressing lines were dip-inoculated with bacterial suspensions of *Pst* DC300 or DC3000 HrcC⁻, 1×10^8 cfu mL^{-1}. After 3 d, or 4 d in the case of DC3000 HrcC⁻, the bacteria were counted (Katagiri *et al.*, 2002). No significant differences in bacterial growth were detected between any of the mutant and wt plants (Fig. S3).

One of the earliest responses of plants to pathogen recognition is the production of ROS. ROS are produced during both PTI and ETI phases of the plant immune response (Torres, 2010). We investigated ROS production after flg22 treatment in knockout and *NPC2*-overexpressing lines. ROS production was significantly higher in four of the six investigated NPC2-OE lines (Fig. 9B, C). All lines with *NPC2* expression higher than four-fold compared to wt showed significantly higher ROS production after flg22 treatment. We speculate that higher ROS production is detectable in the lines that express NPC2 above a certain threshold. ROS production of NPC2-overexpressing plants not treated with flg22 was similar to that of untreated wt plants (Fig. 9C). The *npc2* lines did not differ in ROS production from wt plants (data not shown).

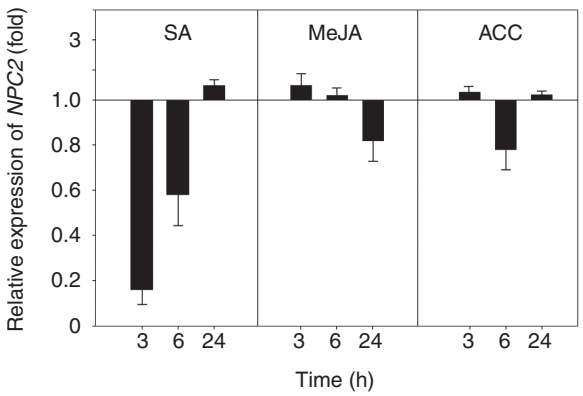

FIG. 7. Analysis of *NPC2* expression after SA, MeJA and ACC treatments. Leaves of 5-week-old Arabidopsis plants were infiltrated with SA (500 μM), MeJA (50 μM) and ACC (5 mM). At 3, 6 and 24 h after infiltration, the transcript levels of the NPC2 gene were measured by quantitative real-time PCR. *SAND* was used as a reference gene. The expression of each gene in water-infiltrated controls was set to 1. The data represent the means ± s.e., $n = 3$ discrete samples from three biological experiments. ACC, 1-aminocyclopropane-1-carboxylic acid; MeJA, methyljasmonic acid; NPC, non-specific phospholipase C; SA, salicylic acid.

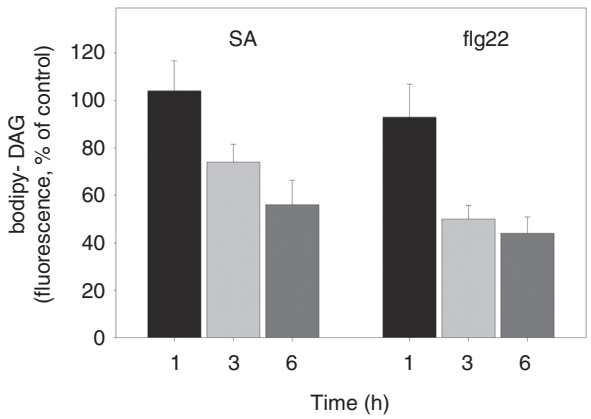

FIG. 8. Effect of flg22 and SA on NPC activity in Arabidopsis protoplasts. Arabidopsis protoplasts were prepared as described in the Material and Methods section. Protoplasts were incubated with flg22 (1 μM) or SA (50 μM) for 1, 3 and 6 h. Bodipy-PC was added to the reaction mixture 30 min before the end of the treatment. At the end of the treatment, lipids were extracted, separated by HP-TLC and quantified. The quantity of bodipy-DAG, the product of NPC activity, in control non-treated protoplasts was set to 100 % at each treatment time. The data represent the means ± s.e. from three independent experiments. DAG; diacylglycerol, SA; salicylic acid.

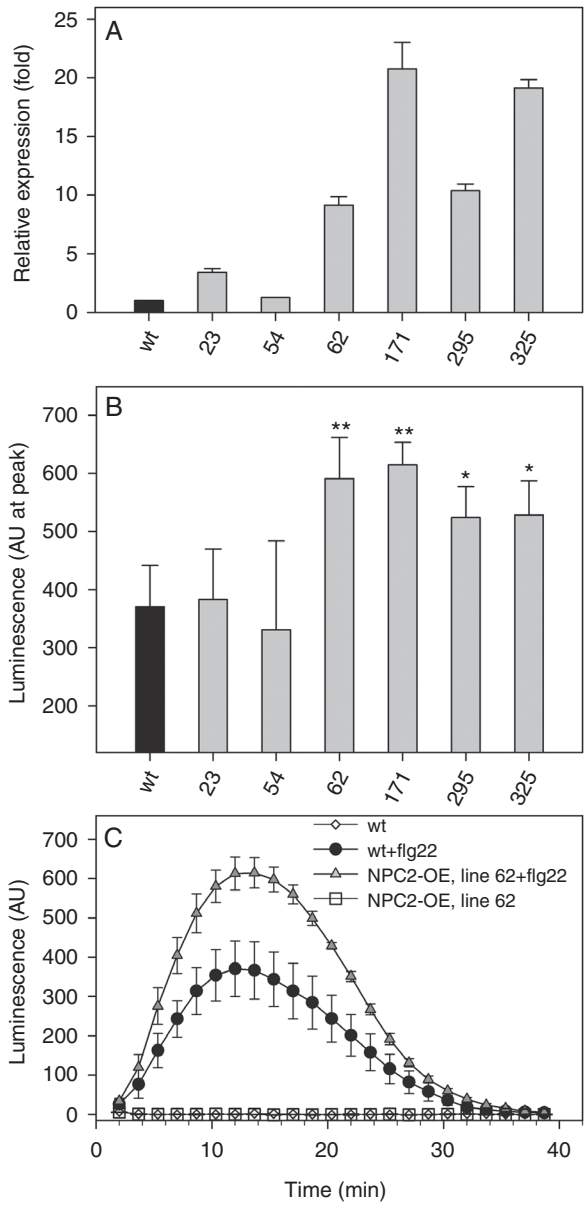

FIG. 9. *NPC2* expression in six NPC2 overexpression lines and ROS production triggered by flg22. (A) The transcript level of *NPC2* was measured by quantitative real-time PCR in Arabidopsis NPC2 overexpression lines (23, 54, 62, 171, 295 and 325). The expression of *NPC2* in wild type plants was set to 1. *SAND* was used as a reference gene. The data represent the means ± s.d., $n = 3$. (B) ROS production (represented by the peak luminescence) of wt and NPC2 overexpression lines 23, 54, 62, 171, 295 and 325 triggered by 100 nM flg22. The data represent the means ± s.e. from four independent experiments. (C) ROS production kinetics. The ROS production kinetics monitored after 40 min in non-treated and 100 nM flg22 treated wt plants and NPC2 overexpressing line 62 plants. The data represent the means ± s.e., n=8 discrete leaf discs. Asterisks denote a significant difference compared to the wt (two-tailed Student's test, $n = 4$, $*P < 0.05$, $**P < 0.01$).

DISCUSSION

NPC2 *encodes a protein with PLC activity, is expressed in a wide range of plant organs and predominantly localizes to GA*

NPC2 belongs to the NPC protein family. NPC1, NPC4 and NPC5 are members of this family that show PLC activity with specificity for major membrane phospholipids, such as PC. Recombinant NPC1, when expressed in *E. coli*, showed activity toward PC (Krčková *et al.*, 2015). Recombinant NPC4 cleaved PC and phosphatidylethanolamine, and this activity was not calcium-dependent. With phosphatidic acid (PA) and phosphatidylinositol 4,5-bisphosphate, no activity was detected (Nakamura *et al.*, 2005). NPC5 was also heterologously expressed in *E. coli*. This protein cleaves PC and phosphatidylethanolamine to produce DAG. When PLC activity was measured using PC as a substrate, NPC4 showed 40-fold higher activity than NPC5 (Gaude *et al.*, 2008). It was also shown that other members of this protein family possess different enzyme activities. Heterologously expressed AtNPC3 has lysophosphatidic acid phosphatase activity (Reddy *et al.*, 2010). We expressed the NPC2 protein in *E. coli*. Of the six Arabidopsis NPCs, NPC1, NPC2 and NPC6 have putative transit peptides at the N-termini that were predicted to be signal peptides (Nakamura *et al.*, 2005; Pokotylo *et al.*, 2013). According to Tan *et al.* (1997), we removed the signal peptide sequence during preparation of the recombinant protein. An enzyme assay with recombinant NPC2 showed cleavage of PC, producing DAG. Substrate specificity and the biochemical characteristics of NPC2 remain unclear and require further study.

Tissue-specific expression patterns revealed GUS staining is consistent with the transcript accumulation pattern obtained from the Genevestigator database (https://genevestigator.com/gv/doc/intro_plant.jsp) (Hruz *et al.*, 2008). In contrast, Peters *et al.* (2010) described very high expression of *NPC2* in siliques compared to other tissues.

NPC2 was predicted to localize to the ER based on the presence of a signal sequence (Pokotylo *et al.*, 2013). In root epidermal cells, we detected weak reticular NPC2:GFP signal, which may in fact correspond with the predicted ER localization. This pattern may on the other hand reflect only the synthesis of the protein on ER while its 'final' localization is in a downstream compartment of the secretory pathway. We observed puncta or aggregated NPC2:GFP signal with higher intensity that co-localized partially with FM4-64-labelled endosomes and to a greater extent with GA cisternae or vesicles marked with MEMB12:mCherry. Because FM4-64 labels the early endosomes or *trans* Golgi network, *trans* Golgi cisternae and vesicles, prevacuolar compartment and tonoplast gradually with increasing time of incubation (Bolte *et al.*, 2004; Malinska *et al.*, 2014) and MEMB12 is localized at *cis* Golgi cisternae and vesicles (Uemura *et al.*, 2004), we suppose that NPC2 is present in both *cis* and *trans* GA and possibly also in the *trans* Golgi network. The function of NPC2 in GA may be connected to its ability to produce DAG. In plants, less knowledge about DAG function has been revealed so far compared with the situation in animal cells (Dong *et al.*, 2012). However, in animal cells, DAG has been shown to be involved in membrane trafficking at the GA (Sarri *et al.*, 2011), DAG is necessary for the proper development of Golgi vesicles and tubules (Asp *et al.*, 2009) and is required for COPI vesicle formation and retrograde (Golgi apparatus to ER) vesicular transport (Fernandez-Ulibarri *et al.*, 2007). Alternatively, DAG produced by NPC2 at the GA may be converted by the action of DAG kinases (Peters *et al.*, 2010) to PA, a known potent second messenger molecule in plants. Such functional coupling would probably require close spatial arrangement. Diacylglycerol kinases DGK1 and DGK2 were found to be localized in ER membranes

(Vaultier *et al.*, 2008), which are functionally tightly connected with the GA. The localization of other DGK isoforms is not known. However, in animal cells one DGK isoform localizes at the GA (Nakano *et al.*, 2012).

The level of NPC2 *transcript is rapidly affected during plant immune responses and correlates with the activation of multiple layers of plant defence systems*

The transcriptional regulation of gene expression is one of the main mechanisms implicated in the guidance of all aspects of plant stress responses. Our qRT-PCR analysis demonstrated that *Psm* infiltration induced a decrease in the *NPC2* transcript level that was rapid, concentration-dependent and steady over a long period (36 h). Not surprisingly, upon encountering a pathogen attack, plants need to quickly rearrange their metabolic fluxes and activate defence systems. This response implies substantial changes to genome expression (Thilmony *et al.*, 2006). The significant reduction in *NPC2* expression after the stimulation of plant defences appears to be specific, and its physiological role is discussed below.

Our results indicate that inhibition of *NPC2* expression is specific and can be directly associated with several components of plant defences: PTI, ETI and SA, a hormone involved in the regulation of responses to biotic stress. The plant PTI system can be efficiently stimulated by the elicitor flg22. In our experiments, *NPC2* expression was rapidly repressed by flg22. The effect of the ETI interaction on *NPC2* expression was tested in two experiments. First, Arabidopsis plants were infiltrated by bacteria that express the AvrRpm1 effector. In another experiment, the AvrRpm1 effector was expressed under an inducible promoter in Arabidopsis plants themselves. In both cases, strong inhibition of *NPC2* expression was observed, suggesting that ETI is similarly effective for the downregulation of *NPC2* expression. The effector AvrRpm1-induced reduction in *NPC2* expression was greater in the wt background compared to *rpm1* and *rpm1 rps2* backgrounds. This observation is consistent with the findings of Kim *et al.* (2009), who demonstrated that AvrRpm1 elicits defence signalling through the Arabidopsis R-proteins RPM1 and RPS2. However, a partial decrease in the *NPC2* transcript level was observed in both *rpm1* and *rpm1 rps2* background plants as well. This result corresponds with the observation of Belkhadir *et al.* (2004), who observed that significant disease-like symptoms were induced following the conditional expression of AvrRpm1 in *rpm1 rps2* plants. This result may signify that redundant mechanisms are implicated during the ETI response that results in the modification of *NPC2* expression.

SA also induced a decrease in the *NPC2* transcript level. SA is known to accumulate in infected leaves and to facilitate the activation of many branches of plant defences (Spoel *et al.*, 2007). *NPC2* expression did not react to MeJA or ACC treatments, indicating that the decrease in *NPC2* transcript may be an important event in the plant reaction to biotrophic, but not to necrotrophic, pathogens. These data are also consistent with the physiological roles of SA and MeJA hormones in orchestrating antagonistic branches of plant immune responses (Thaler *et al.*, 2012).

Thus, our results suggest that the downregulation of *NPC2* expression is likely to be a result of the activity of multiple plant defence systems. PTI responses are dominant during the early part of the response to biotic stress, whereas ETI signalling is likely to act in concert with an overall increased SA level to downregulate the *NPC2* transcript level at later phases of infection.

Overexpression of NPC2 *results in overproduction of ROS after flg22 treatment*

Our results showed that overexpression of NPC2 led to higher accumulation of ROS after flg22 treatment. Higher activity of NPC2 may result in higher PA content via DAG conversion to PA by DAG kinase (Arisz *et al.*, 2009). PA is known to promote ROS production by its direct interaction with NADPH oxidase RbohD and RbohF (Zhang *et al.*, 2009). Whether this mechanism functions during Arabidopsis – *P. syringae* interaction needs to be investigated in future.

Possible function of NPC during plant–pathogen interactions

The role of NPC2 in defence reactions may be ascribed to the production of DAG and phosphocholine (Pchol) molecules as well as to changes in PC content in the membranes. The role of Pchol, which is produced by NPC, is currently unknown in plants. However, bacteria often stimulate nutrient release into the apoplast and use host-derived precursors (choline) to synthesize PC required for pathogenicity as a part of host mimicry (de Rudder *et al.*, 1999). Bacteria also use choline as a source of nitrogen and as an osmoprotectant. The addition of choline significantly increases tabtoxin production in *P. syringae*. More importantly, the activity of phosphocholine phosphatase (conserved in all *Pseudomonas* species) was also induced, suggesting that the Pchol produced by NPC may be readily used by bacteria during infection (Gallarato *et al.*, 2012; Chen *et al.*, 2013). These results suggest that the inhibition of NPC2 on the transcriptional level might limit the availability of soluble Pchol for invading bacteria.

DAG is known to be implicated in the regulation of many cell processes (Dong *et al.*, 2012). Among these processes are defence-related phytoalexin (Kurosaki *et al.*, 1987) and ROS production (Yamaguchi *et al.*, 2005). DAG is also known to be converted to PA in plants by DGK (Arisz *et al.*, 2009). PA itself is a well-known signalling molecule that is typically produced from PLD activity (Kolesnikov *et al.*, 2012; Zhao, 2015). Therefore, one of the possible explanations for *NPC2* downregulation is an effort by the plant cell to preserve the level of metabolically available PC in the membranes as PLD substrate. Thus, membrane properties will remain unaffected even in the case of intense stress-induced PLD activation.

Furthermore, both PA and DAG influence the structure and dynamics of membranes. For example, DAG, when concentrated in small membrane areas, can affect membrane curvature and induce unstable, asymmetric regions in membrane bilayers. These features are essential for membrane fusion and fission processes and may influence membrane rigidity (Carrasco and Mérida, 2007; Haucke and Di Paolo, 2007). The fact that PA, which may be an indirect product of NPC activity, affects vesicle trafficking-related processes (Hong *et al.*, 2016) is of

special interest, particularly in view of the fact that NPC2 is localized to the GA.

SUPPLEMENTARY DATA

Supplementary data are available online at www.aob.oxfordjournals.org and consist of the following. Fig. S1. Expression pattern of *NPC2* in *Pseudomonas syringae* pv. *maculicola*-treated plants. Fig. S2. Analysis of NPC2 expression in Arabidopsis inoculated with *Psm* and *Pst* wild type strains and with the mutant bacteria *Psm* AvrRpm1, *Pst COR*$^-$ and *Pst hrcC*$^-$. Fig. S3. Infection of NPC2 mutants with *Pseudomonas syringae*. Table S1. Description of microarray experimental conditions used for *NPC2* transcriptome analysis.

ACKNOWLEDGEMENTS

The authors thank Kateřina Vltavská and Kateřina Raková for their excellent technical assistance. We are grateful to David Mackey (Department of Molecular Genetics, The Ohio State University, USA) for providing the Arabidopsis Dex:AvrRpm1 Col 0, Dex:AvrRpm1 *rpm1.3*, Dex:AvrRpm1 *rpm1.3 rps2-101C* and *rpm1.3*, *rpm1.3 rps2-101C* null mutant plants. This work was supported by the Czech Science Foundation grant no. P501/12/1942.

LITERATURE CITED

Alonso JM. 2003. Genome-wide insertional mutagenesis of *Arabidopsis thaliana*. *Science* **301**: 653–657.

Andersson MX, **Larsson KE**, **Tjellström H**, **Liljenberg C**, **Sandelius AS. 2005**. Phosphate-limited oat. The plasma membrane and the tonoplast as major targets for phospholipid-to-glycolipid replacement and stimulation of phospholipases in the plasma membrane. *Journal of Biological Chemistry* **280**: 27578–27586.

Andersson MX, **Kourtchenko O**, **Dangl JL**, **Mackey D**, **Ellerström M. 2006**. Phospholipase-dependent signalling during the AvrRpm1- and AvrRpt2-induced disease resistance responses in *Arabidopsis thaliana*. *Plant Journal* **47**: 947–959.

Arisz SA, **Testerink C**, **Munnik T. 2009**. Plant PA signaling via diacylglycerol kinase. *Biochimica et Biophysica Acta - Molecular and Cell Biology of Lipids* **1791**: 869–875.

Asp L, **Kartberg F**, **Fernandez-Rodriguez J**, ***et al*. 2009**. Early stages of Golgi vesicle and tubule formation require diacylglycerol. *Molecular Biology of the Cell* **20**: 780–790.

Belkhadir Y, **Nimchuk Z**, **Hubert DA**, **Mackey D**, **Dangl JL. 2004**. Arabidopsis RIN4 negatively regulates disease resistance mediated by RPS2 and RPM1 downstream or independent of the NDR1 signal modulator and is not required for the virulence functions of bacterial type III effectors AvrRpt2 or AvrRpm1. *Plant Cell* **16**: 2822–2835.

Bolte S, **Talbot C**, **Boutte Y**, **Catrice O**, **Read ND**, **Satiat-Jeunemaitre B. 2004**. FM-dyes as experimental probes for dissecting vesicle trafficking in living plant cells. *Journal of Microscopy* **214**: 159–173.

Bradford MM. 1976. A rapid and sensitive method for the quantification of microgram quantities of protein utilizing the principle of protein-dye binding. *Analytical Biochemistry* **72**: 248–254.

Cao H, **Zhuo L**, **Su Y**, **Sun L**, **Wang X. 2016**. Non-specific phospholipase C1 affects silicon distribution and mechanical strength in stem nodes of rice. *Plant Journal* **86**: 308–321.

Carrasco S, **Mérida I. 2007**. Diacylglycerol, when simplicity becomes complex. *Trends in Biochemical Sciences* **32**: 27–36.

Chen C, **Li S**, **McKeever DR**, **Beattie GA. 2013**. The widespread plant-colonizing bacterial species *Pseudomonas syringae* detects and exploits an extracellular pool of choline in hosts. *Plant Journal* **75**: 891–902.

Clough SJ, **Bent AF. 1998**. Floral dip: a simplified method for *Agrobacterium*-mediated transformation of *Arabidopsis thaliana*. *Plant Journal* **16**: 735–743.

Czechowski T, **Stitt M**, **Altmann T**, **Udvardi MK**, **Scheible WR. 2005**. Genome-wide identification and testing of superior reference genes for transcript normalization in Arabidopsis. *Plant Physiology* **139**: 5–17.

de Jonge R, **van Esse HP**, **Kombrink A**, ***et al*. 2010**. Conserved fungal LysM effector Ecp6 prevents chitin-triggered immunity in plants. *Science* **329**: 953–5.

de Rudder KEE, **Sohlenkamp C**, **Geiger O. 1999**. Plant-exuded choline is used for rhizobial membrane lipid biosynthesis by phosphatidylcholine synthase. *Journal of Biological Chemistry* **274**: 20011–20016.

Dong W, **Lv H**, **Xia G**, **Wang M. 2012**. Does diacylglycerol serve as a signaling molecule in plants? *Plant Signaling & Behavior* **7**: 1–4.

Fernandez-Ulibarri I, **Vilella M**, **Lazaro-Dieguez F**, ***et al*. 2007**. Diacylglycerol is required for the formation of COPI vesicles in the Golgi-to-ER transport pathway. *Molecular Biology of the Cell* **18**: 3250–3263.

Gallarato LA, **Primo ED**, **Lisa ÁT**, **Garrido MN. 2012**. Choline promotes growth and tabtoxin production in a *Pseudomonas syringae* strain. *Advances in Microbiology* **2**: 327–331.

Gaude N, **Nakamura Y**, **Scheible WR**, **Ohta H**, **Dormann P. 2008**. Phospholipase C5 (NPC5) is involved in galactolipid accumulation during phosphate limitation in leaves of Arabidopsis. *Plant Journal* **56**: 28–39.

Geldner N, **Denervaud-Tendon V**, **Hyman DL**, **Mayer U**, **Stierhof Y-D**, **Chory J. 2009**. Rapid, combinatorial analysis of membrane compartments in intact plants with a multicolor marker set. *Plant Journal* **59**: 169–178.

Grant MR, **Godiard L**, **Straube E**, ***et al*. 1995**. Structure of the *Arabidopsis RPM1* gene enabling dual specificity disease resistance. *Science* **269**: 843–846.

Haucke V, **Di Paolo G. 2007**. Lipids and lipid modifications in the regulation of membrane. *Current Opinion in Cell Biology* **19**: 426–435.

Hong Y, **Zhao J**, **Guo L**, ***et al*. 2016**. Plant phospholipases D and C and their diverse functions in stress responses. *Progress in Lipid Research* **62**: 55–74.

Hruz T, **Laule O**, **Szabo G**, ***et al*. 2008**. Genevestigator V3: A reference expression database for the meta-analysis of transcriptomes. *Advances in Bioinformatics*, 2008: Article ID 420747.

Janda M, **Planchais S**, **Djafi N**, ***et al*. 2013**. Phosphoglycerolipids are master players in plant hormone signal transduction. *Plant Cell Reports* **32**: 839–851.

Janda M, **Sasek V**, **Chmelarova H**, ***et al*. 2015**. Phospholipase D affects translocation of NPR1 to the nucleus in Arabidopsis thaliana. *Frontiers in Plant Science* **6**: 59.

Jefferson RA, **Kavanagh TA**, **Bevan MW. 1987**. GUS fusions: β-glucuronidase as a sensitive and versatile gene fusion marker in higher plants. *EMBO Journal* **6**: 3901–3907.

Karimi M, **Inze D**, **Depicker A. 2002**. GATEWAY^{TM} vectors for *Agrobacterium*-mediated plant transformation. *Trends in Plant Science* **7**: 193–195.

Katagiri F, **Thilmony R**, **He SY. 2002**. The *Arabidopsis thaliana-Pseudomonas syringae* interaction. *The Arabidopsis Book* **1**: e0039.

Kim MG, **Geng X**, **Lee SY**, **Mackey D. 2009**. The *Pseudomonas syringae* type III effector AvrRpm1 induces significant defenses by activating the Arabidopsis nucleotide-binding leucine-rich repeat protein RPS2. *Plant Journal* **57**: 645–653.

Kocourková D, **Krčková Z**, **Pejchar P**, ***et al*. 2011**. The phosphatidylcholine-hydrolyzing phospholipase C NPC4 plays a role in response of *Arabidopsis* roots to salt stress. *Journal of Experimental Botany* **62**: 3753–3763.

Kolesnikov YS, **Nokhrina KP**, **Kretynin SV**, ***et al*. 2012**. Molecular structure of phospholipase D and regulatory mechanisms of its activity in plant and animal cells. *Biochemistry (Moscow)* **77**: 1–14.

Krčková Z, **Brouzdová J**, **Danek M**, ***et al*. 2015**. Arabidopsis non-specific phospholipase C1: Characterisation and its involvement in response to heat stress. *Frontiers in Plant Science,* **6**: 928.

Krinke O, **Flemr M**, **Vergnolle C**, ***et al*. 2009**. Phospholipase D activation is an early component of the salicylic acid signaling pathway in Arabidopsis cell suspensions. *Plant Physiology* **150**: 424–436.

Kurosaki F, **Tsurusawa Y**, **Nishi A. 1987**. Breakdown of phosphatidylinositol during the elicitation of phytoalexin production in cultured carrot cells. *Plant Physiology* **85**: 601–604.

La Camera S, **Geoffroy P**, **Samaha H**, ***et al*. 2005**. A pathogen-inducible patatin-like lipid acyl hydrolase facilitates fungal and bacterial host colonization in Arabidopsis. *Plant Journal* **44**: 810–825.

Malinska K, **Jelinkova A**, **Petrasek J. 2014**. The use of FM dyes to analyze plant endocytosis. In: Otegui MS, ed. *Plant Endosomes: Methods and Protocols*. New York: Humana Press.

Mindrinos M, **Katagiri F**, **Yu G-L**, **Ausubel FM. 1994**. The A. thaliana disease resistance gene *RPS2* encodes a protein containing a nucleotide-binding site and leucine-rich repeats. *Cell* **78**: 1089–1099.

Nakagawa T, **Kurose T**, **Hino T**, ***et al***. **2007**. Development of series of gateway binary vectors, pGWBs, for realizing efficient construction of fusion genes for plant transformation. *Journal of Bioscience and Bioengineering* **104**: 34–41.

Nakamura Y, **Awai K**, **Masuda T**, **Yoshioka Y**, **Takamiya K**, **Ohta H. 2005**. A novel phosphatidylcholine-hydrolyzing phospholipase C induced by phosphate starvation in *Arabidopsis*. *Journal of Biological Chemistry* **280**: 7469–7476.

Nakano T, **Hozumi Y**, **Goto K**, **Wakabayashi I. 2012**. Involvement of diacylglycerol kinase γ in modulation of iNOS synthesis in Golgi apparatus of vascular endothelial cells. *Naunyn-Schmiedebergs Archives of Pharmacology* **385**: 787–795.

Pejchar P, **Martinec J. 2015**. Aluminium ions alter the function of non-specific phospholipase C through the changes in plasma membrane physical properties. *Plant Signaling & Behavior* **10**: e1031938.

Pejchar P, **Potocký M**, **Novotná Z**, ***et al***. **2010**. Aluminium ions inhibit the formation of diacylglycerol generated by phosphatidylcholine-hydrolysing phospholipase C in tobacco cells. *New Phytologist* **188**: 150–160.

Pejchar P, **Scherer GFE**, **Martinec J. 2013**. Assaying nonspecific phospholipase C activity. In: Munnik T, Heilmann I, eds. *Plant Lipid Signaling Protocols*. New York: Humana Press.

Pejchar P, **Potocky M**, **Krckova Z**, **Brouzdova J**, **Danek M**, **Martinec J. 2015**. Non-specific phospholipase C4 mediates response to aluminum toxicity in *Arabidopsis thaliana*. *Frontiers in Plant Science* **6**: 66.

Peters C, **Li M**, **Narasimhan R**, **Roth M**, **Welti R**, **Wang XM. 2010**. Nonspecific phospholipase C NPC4 promotes responses to abscisic acid and tolerance to hyperosmotic stress in *Arabidopsis*. *Plant Cell* **22**: 2642–2659.

Peters C, **Kim S-C**, **Devaiah S**, **Li M**, **Wang X. 2014**. Non-specific phospholipase C5 and diacylglycerol promote lateral root development under mild salt stress in Arabidopsis. *Plant, Cell & Environment* **37**: 2002–13.

Pfaffl MW. 2001. A new mathematical model for relative quantification in real-time RT-PCR. *Nucleic Acids Research* **29**: e45.

Pokotylo I, **Pejchar P**, **Potocký M**, ***et al***. **2013**. The plant non-specific phospholipase C gene family. Novel competitors in lipid signalling. *Progress in Lipid Research* **52**: 62–79.

Profotová B, **Burketová L**, **Novotná Z**, **Martinec J**, **Valentová O. 2006**. Involvement of phospholipases C and D in early response to SAR and ISR inducers in *Brassica napus* plants. *Plant Physiology and Biochemistry* **44**: 143–151.

Reddy VS, **Rao DKV**, **Rajasekharan R. 2010**. Functional characterization of lysophosphatidic acid phosphatase from *Arabidopsis thaliana*. *Biochimica et Biophysica Acta - Molecular and Cell Biology of Lipids* **1801**: 455–461.

Sarri E, **Sicart A**, **Lazaro-Dieguez F**, **Egea G. 2011**. Phospholipid synthesis participates in the regulation of diacylglycerol required for membrane trafficking at the Golgi complex. *Journal of Biological Chemistry* **286**: 28632–28643.

Sasek V, **Janda M**, **Delage E**, ***et al***. **2014**. Constitutive salicylic acid accumulation in pi4kIII beta 1 beta 2 Arabidopsis plants stunts rosette but not root growth. *New Phytologist* **203**: 805–816.

Senthil-Kumar M, **Mysore KS. 2013**. Nonhost resistance against bacterial pathogens: retrospectives and prospects. *Annual Review of Phytopathology* **51**: 407–427.

Scherer GFE, **Paul RU**, **Holk A**, **Martinec J. 2002**. Down-regulation by elicitors of phosphatidylcholine-hydrolyzing phospholipase C and up-regulation of phospholipase A in plant cells. *Biochemical and Biophysical Research Communications* **293**: 766–770.

Singh A, **Kanwar P**, **Pandey A**, ***et al***. **2013**. Comprehensive genomic analysis and expression profiling of phospholipase C gene family during abiotic stresses and development in rice. *PLoS ONE*, **8**: e62494.

Spoel SH, **Dong X. 2012**. How do plants achieve immunity? Defence without specialized immune cells. *Nature Reviews Immunology* **12**: 89–100.

Spoel SH, **Johnson JS**, **Dong X. 2007**. Regulation of tradeoffs between plant defenses against pathogens with different lifestyles. *Proceedings of the National Academy of Sciences of the United States of America* **104**: 18842–18847.

Tan CA, **Hehir MJ**, **Roberts MF. 1997**. Cloning, overexpression, refolding, and purification of the nonspecific phospholipase C from *Bacillus cereus*. *Protein Expression and Purification* **10**: 365–372.

Thaler JS, **Humphrey PT**, **Whiteman NK. 2012**. Evolution of jasmonate and salicylate signal crosstalk. *Trends in Plant Science* **17**: 260–270.

Thilmony R, **Underwood W**, **He SY. 2006**. Genome-wide transcriptional analysis of the *Arabidopsis thaliana* interaction with the plant pathogen *Pseudomonas syringae* pv. *tomato* DC3000 and the human pathogen *Escherichia coli* O157:H7. *Plant Journal* **46**: 34–53.

Tjellström H, **Andersson MX**, **Larsson KE**, **Sandelius AS. 2008**. Membrane phospholipids as a phosphate reserve: the dynamic nature of phospholipid-to-digalactosyl diacylglycerol exchange in higher plants. *Plant Cell and Environment* **31**: 1388–1398.

Torres MA. 2010. ROS in biotic interactions. *Physiologia Plantarum* **138**: 414–429.

Uemura T, **Ueda T**, **Ohniwa RL**, **Nakano A**, **Takeyasu K**, **Sato MH. 2004**. Systematic analysis of SNARE molecules in *Arabidopsis*: Dissection of the post-Golgi network in plant cells. *Cell Structure and Function* **29**: 49–65.

Vaultier M-N, **Cantrel C**, **Guerbette F**, ***et al***. **2008**. The hydrophobic segment of *Arabidopsis thaliana* cluster I diacylglycerol kinases is sufficient to target the proteins to cell membranes. *FEBS Letters* **582**: 1743–1748.

Viehweger K, **Schwartze W**, **Schumann B**, **Lein W**, **Roos W. 2006**. The Gα protein controls a pH-dependent signal path to the induction of phytoalexin biosynthesis in *Eschscholzia californica*. *Plant Cell* **18**: 1510–1523.

Vossen JH, **Abd-El-Haliem A**, **Fradin EF**, ***et al***. **2010**. Identification of tomato phosphatidylinositol-specific phospholipase-C (PI-PLC) family members and the role of PLC4 and PLC6 in HR and disease resistance. *Plant Journal* **62**: 224–239.

Wang C, **Zien CA**, **Afitlhile M**, **Welti R**, **Hildebrand DF**, **Wang X. 2000**. Involvement of phospholipase D in wound-induced accumulation of jasmonic acid in Arabidopsis. *Plant Cell* **12**: 2237–2246.

Wimalasekera R, **Pejchar P**, **Holk A**, **Martinec J**, **Scherer GFE. 2010**. Plant phosphatidylcholine-hydrolyzing phospholipases C NPC3 and NPC4 with roles in root development and brassinolide signalling in *Arabidopsis thaliana*. *Molecular Plant* **3**: 610–625.

Wu FH, **Shen SC**, **Lee LY**, **Lee SH**, **Chan MT**, **Lin CS. 2009**. Tape-*Arabidopsis* Sandwich - a simpler *Arabidopsis* protoplast isolation method. *Plant Methods* **5**: 16.

Yamaguchi T, **Minami E**, **Ueki J**, **Shibuya N. 2005**. Elicitor-induced activation of phospholipases plays an important role for the induction of defense responses in suspension-cultured rice cells. *Plant and Cell Physiology* **46**: 579–587.

Yamaguchi T, **Kuroda M**, **Yamakawa H**, ***et al***. **2009**. Suppression of a phospholipase D gene, *OsPLDβ1*, activates defense responses and increases disease resistance in rice. *Plant Physiology* **150**: 308–319.

Yamaguchi Y, **Huffaker A**, **Bryan AC**, **Tax FE**, **Ryan CA. 2010**. PEPR2 is a second receptor for the Pep1 and Pep2 peptides and contributes to defense responses in *Arabidopsis*. *Plant Cell* **22**: 508–522.

Zhang B, **Wang Y**, **Liu JY. 2017**. Genome-wide identification and characterization of phospholipase C gene family in cotton (*Gossypium* spp.). *Science China Life Sciences*. https://doi.org/10.1007/s11427-017-9053-y

Zhang YY, **Zhu HY**, **Zhang Q**, ***et al***. **2009**. Phospholipase Dα1 and phosphatidic acid regulate NADPH oxidase activity and production of reactive oxygen species in ABA-mediated stomatal closure in *Arabidopsis*. *Plant Cell* **21**: 2357–2377.

Zhao J. 2015. Phospholipase D and phosphatidic acid in plant defence response: from protein-protein and lipid-protein interactions to hormone signalling. *Journal of Experimental Botany* **66**: 1721–1736.

Zhao J, **Devaiah SP**, **Wang C**, **Li M**, **Welti R**, **Wang X. 2013**. Arabidopsis phospholipase Dβ1 modulates defense responses to bacterial and fungal pathogens. *New Phytologist* **199**: 228–240.